

A Novel Foaming Approach to Prepare Porous Superabsorbent Poly(sodium acrylic acid) Resins

Jianshe Bao, Si Chen, Bozhen Wu, Meng Ma, Yanqin Shi, Xu Wang

College of Chemical Engineering and Materials Science, Zhejiang University of Technology, Hangzhou 310014, China

Correspondence to: X. Wang (E-mail: wangxu@zjut.edu.cn)

ABSTRACT: A system composed of surfactant and foam stabilizer is used in preparing porous superabsorbent resins (SARs) of poly(sodium acrylic acid) (PAA-Na), which is obtained by free-radical solution polymerization of partially neutralized acrylic acid with mechanical agitation of eggbeater. Different types of surfactant, including anionic surfactant sodium *n*-dodecyl benzene sulfate (SDBS), cationic surfactant cetyltrimethyl ammonium bromide, and nonionic surfactant alkylphenols poly(oxyethylene) (OP-10), are used as blowing agent to produce pores by mechanical agitation, and triethanolamine (TEA) is used to act as foam stabilizer agent. The results show that a synergistic effect of SDBS with TEA is obtained and the packing density is decreased, which could be proved by the clearly porous morphology, and the water absorbing capacity of SARs is enhanced. As a result, such method can get PAA-Na SARs without any organic solvents, which provides an environmentally beneficial way to prepare SARs for hygiene and biomedical products. © 2014 Wiley Periodicals, Inc. *J. Appl. Polym. Sci.* **2015**, *132*, 41298.

KEYWORDS: foams; porous materials; resins; surfactants; swelling

Received 13 January 2014; accepted 13 July 2014

DOI: 10.1002/app.41298

INTRODUCTION

Superabsorbent resins (SARs) are a kind of slightly cross-linked functional materials that can absorb large quantities of water or other physiological fluids without any disruption and have extensive applications in various areas such as agriculture, horticulture, sanitary napkins, disposable nappies, and other fields.^{1–4} In the development of new SARs, high water absorption, fast swelling rate, and good gel strength are especially desired. Among these properties, swelling rate is most important because it restricts applications of SARs in almost every field. However, traditional SARs such as acrylic-acrylamide-based SAR⁵ often takes hours to reach the swelling equilibrium because of absorbing water through diffusion. Therefore, many researchers have focused on improving the swelling rate of SARs for expanding their applications. In principle, a fast swelling rate is due to absorbing water by capillary force and diffusion rather than by simple diffusion, and the formed pores in the microstructure could be channels for capillary.⁶ So creating of porous microstructure allows faster diffusion of water into the polymeric network by reducing osmotic pressure. Many methods of creating porous microstructure have already been reported in the literatures, including phase separation technique,⁷ freeze-drying method,⁸ the foaming technique,⁹ and water-soluble porogens.¹⁰ However, most of these methods are not suitable for industrial

production. The phase separation technique is not much control over the porosity of the porous SARs. The freeze-drying method could not use widely due to high cost. The pore size of SARs depends on the size of porogens, and it needs a large quantity of water to remove the porogens when using the water-soluble porogens. All those disadvantages have been described in detail by Chen et al.,⁶ and the contradiction between controlled porosity and the convenience of pore-foaming technique has still not been solved. In this article, a physical foaming method using surfactant as foaming agent under fiercely agitation with eggbeater was first reported, SARs with porous microstructure was obtained with high water absorption and fast swelling rate, without using any organic solvent during the process of polymerization and post-treatment. As a result, an environmentally beneficial way to prepare SARs for hygiene or biomedical products is realized and this environmental friendly method has the possibility to achieve the goal of industrial production.

Considering the surfactant-polymer mixtures with nontrivial surface rheological property of low surfactant concentration viscoelasticity and high surfactant concentration fluxility,¹¹ low concentration of surfactant was chosen to prevent bubbles from disappearing. Although in viscoelastic solution, the surfactant can self-assembly into micelles to act as a pore template to generate porous microstructure in aqueous environment¹² with the

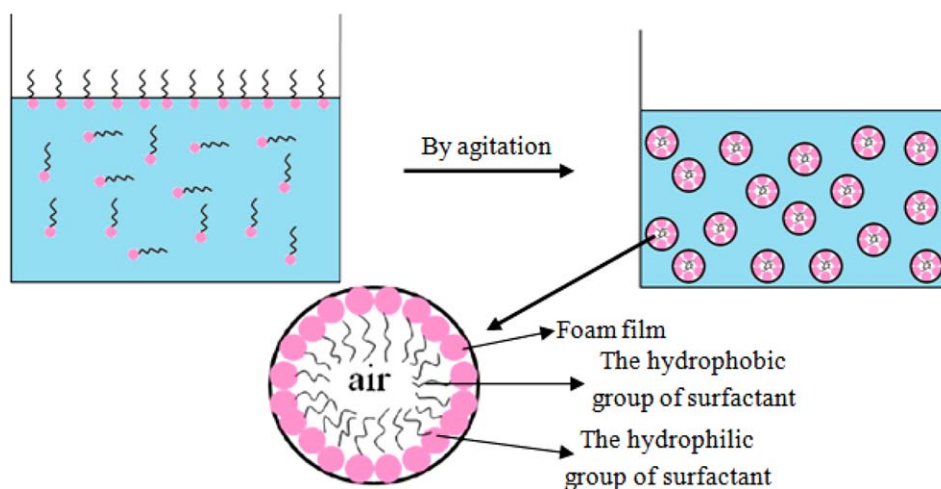
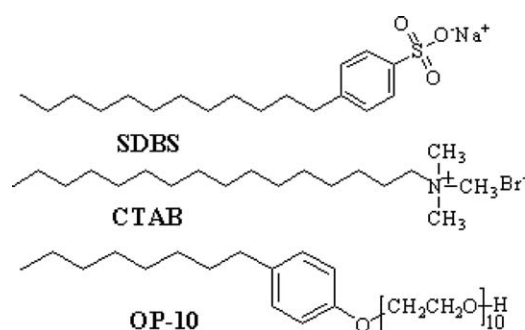


Figure 1. Schematic presentation of the adsorption layers formed in the process of foam formation in the case of surfactant. [Color figure can be viewed in the online issue, which is available at wileyonlinelibrary.com.]

help of acutely mechanical agitation through eggbeater. The surfactant is comprising of two opposite groups, including the hydrophilic group which is toward the solution and the hydrophobic group toward air, so the surfactant can self-assemble to form foams, and it would form foam film in the gas–liquid interface (as shown in Figure 1). The stability of the formed bubbles is actually influenced by many factors, including the viscosity of solution, the charge density of polymer,¹³ the concentration of electrolyte,¹⁴ the length of surfactant tails,¹⁵ and the property of foam film, etc. So only relying on the surfactant concentration could not always maintain the foam stability. In this article, triethanolamine (TEA) was introduced as foam stabilizer, and a special synergistic effect was obtained to increase the stability of foam by increasing the strength and viscosity of the foam film, which resulted from the amphiprotic of the surfactant and prolong the existence time of bubbles by decreasing the drainage speed from the internal and closing to the surface of bubbles.

In order to study such special synergistic effect in detail, three different types of surfactant including anionic surfactant sodium *n*-dodecyl benzene sulfate (SDBS), cationic surfactant cetyltrimethyl ammonium bromide (CTAB), and nonionic surfactant alkylphenols poly(oxyethylene) (OP-10) were introduced in the process of polymerization reaction, and the porous morphology, water absorption ability, swelling rate, and packing density were investigated through water absorption test, swelling rate test, packing density, and scanning electron microscope (SEM), respectively. From the results, we could find out that anionic surfactant SDBS has the best effect on enhancing the resulting water absorption capacity of poly(sodium acrylic acid) (PAA-Na) resins, and the water absorption was 466 g/g, whereas the number was 395 g/g of the resin without adding surfactant. The water absorption could even increase to 543 g/g in the system of surfactant and foam stabilizer and the swelling rate was also obviously enhanced by adding foam stabilizer. The prepared porous PAA-Na resins that possess high water absorption and fast swelling rate show great potential in various pharmaceutical and biomedical applications.



Scheme 1. The structure of the surfactants SDBS, CTAB, and OP-10 used in this study.

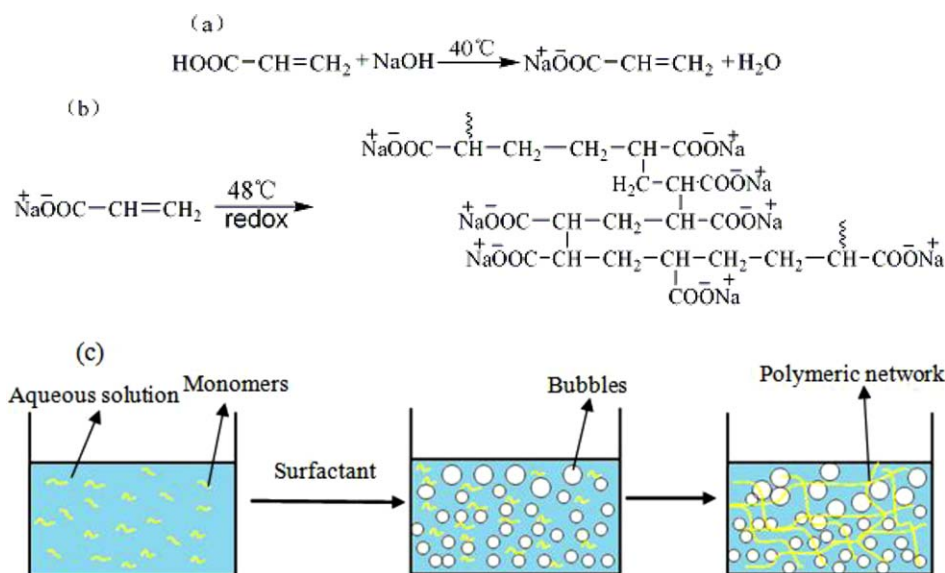
EXPERIMENTAL

Materials

Acrylic acid (AA, 98%), inner crosslinker (AR), and redox initiator (AR) used in this work were supplied by Zhejiang Satellite Petro Chemical Co. (Zhejiang, China). SDBS (AR), CTAB (AR), and TEA (AR) used in this study were all purchased from Aladdin Reagent Co. (Shanghai, China) and used as received and the structures of which were shown in Scheme 1. Other agents used were of analytical grade and all solutions were prepared with distilled water.

The Synthesis of Poly(sodium acrylic acid)

Sodium hydroxide (44.4 g NaOH) was dissolved in 100 mL distilled water in a 500 mL beaker in 40°C water bath equipped with a 100 mL constant pressure funnel and a thermometer to monitor the temperature of the entire reaction. AA (100 mL) was added into NaOH solution [Scheme 2(a)] dropwise through a constant pressure funnel. Then, the inner crosslinker (0.8 mL) was added into the monomer mixture. The appropriate amount of surfactant and foam stabilizer dissolved in 10 mL water was added to the mixture. At the same time, the eggbeater with a speed of 15,000 rpm was used to produce a large amount of bubbles [Scheme 2(c)]. Then, the system was heated to 48°C. After that, 1.6 g 10 wt % aqueous solution of redox



Scheme 2. Proposed mechanism for the formation of porous PAA-Na resins, (a) the neutralization process of AA, (b) the polymerization process of partially neutralized AA, and (c) the process of the interaction of PAA-Na resin and foaming system. [Color figure can be viewed in the online issue, which is available at wileyonlinelibrary.com.]

initiator (the proportion of oxidation and reduction initiator was 1 : 1) was separately added to the mixture. The temperature was increased rapidly as well as the viscosity of the reaction mixture due to the rapid polymerization process [Scheme 2(b)]. The bubbles were wrapped in the polymeric network, which has shown in Scheme 2(c). The resulting hydrogels were washed thoroughly with methanol for several times to remove unreacted monomers or surfactant for the Fourier transform infrared (FTIR) spectroscopy test. And the whole polymerization process in the air. The hydrogels were removed from the beater, cut into bulk, and dried in an air-oven at 100°C for 5 h. Dried products were grinding with a minigrinder and screened 30–80 mesh (187–613 μm) particles before testing.

The comparable nonporous PAA-Na without any surfactant or foam stabilizer was prepared by a similar procedure with surfactant-added samples. The nonporous, SDBS-added, OP-added, and CTAB-added samples were designated as M1, M2, M3, and M4, respectively. Adding foam stabilizer with surfactant SDBS sample was marked as M5. Details of these formulas in detail were shown in Table I.

Packing Density Test

The dried and screened samples were naturally fallen into a known volume and weight container by a self-made funnel, and then, the redundant part was carefully removed using a ruler

without pressing. The packing density ρ was calculated by the following eq. (1):

$$\rho = \frac{m_2 - m_1}{V} \quad (1)$$

where m_2 is the weight of the container filled with samples (g) and m_1 is the weight of the empty container, V is the volume of the container. Each test was repeated five times to obtain the mean value ρ with the error range less than 5%.

Water Absorption Test

The water absorption of PAA-Na was determined by a conventional method: 0.20 g dried samples were immersed in 500 mL distilled water at room temperature. The excess water in the swollen samples was then filtered out by sieve and the samples were allowed to stand for 10 min to exclude the remaining water. The water absorption (Q_{eq} , g/g) was calculated by the following eq. (2):

$$Q_{\text{eq}} = \frac{m_2 - m_1}{m_1} \quad (2)$$

where m_2 is the weight of swollen samples (g) and m_1 is the weight of dried samples (g). Each test was repeated five times to obtain the mean value Q_{eq} with the error range less than 5%.

Swelling Rate Test

The swelling rate of PAA-Na was measured as follows: 0.10 g dried samples were soaked in 200 mL distilled water. At

Table I. The Surfactant and SDBS with TEA of the Samples M1, M2, M3, M4, and M5

Samples	M1	M2	M3	M4	M5
Surfactants	Surfactant free	SDBS	OP-10	CTAB	SDBS/TEA
The surfactant amount (mmol)	0	3	3	3	3/3

Note: Other additives have described are the same, including the types and amount.

consecutive time intervals, the swelling degree (Q_t) of PAA-Na at a given time t (s) was measured by weighing the swollen (m_2) and the dried samples (m_1) according to Eq. (2).

Fourier Transform Infrared

FTIR spectroscopy was measured on a Nicolet NEXUS FTIR 6700 infrared spectrophotometer in 4000–400 cm^{-1} region using KBr pellets.

Scanning Electron Microscope

The morphologies of the different samples were examined using a Hitachi-S4700, Japan SEM instrument after coating the samples with gold film.

RESULT AND DISCUSSION

Infrared Spectra

Figure 2 shows FTIR spectra of M1, M2, M3, M4, and M5, respectively. The changes in the structure of PAA-Na were observed in the case of surfactant-added samples. The peaks appearing around 2865–2850 cm^{-1} can be assigned to the $-\text{CH}_2-$ symmetric stretching vibration of surfactant molecules.¹¹ It showed that surfactant can be acted as a foam template for the formation of pore structure. For the FTIR spectra of M, the broad absorption peaks at about 3420 cm^{-1} can be ascribed to the O–H stretching vibration of PAA-Na and the bonding water molecules. And the peaks at 2940 cm^{-1} and 1268 cm^{-1} can be assigned to the C–H stretching and bending vibration. The absorption bands at 1730–1722 cm^{-1} is the C=O asymmetrical stretching vibration, at 1573–1560 cm^{-1} can be attributed to the $-\text{COO}$ asymmetrical stretching of $-\text{COO}^-$ groups and at 1450–1400 cm^{-1} can be attributed to the $-\text{COO}$ symmetrical stretching of $-\text{COO}^-$ groups. The peaks at 1169 cm^{-1} and 1033 cm^{-1} correspond to C–C and C–O stretching vibration. So, we prepared the PAA-Na resins, and the new peak of 2865–2850 cm^{-1} could be proved that the surfactants could be a foam agent to produce the porous microstructure acting on the resins.

The Influence of Surfactant and the Foam Stabilizer with Surfactant on the Morphology of M1, M2, M3, M4, and M5

The SEM micrographs of the dried samples of M1, M2, M3, M4, and M5 are shown in Figure 3. It gave a clear image of surface morphology from screened particles. The samples M1 and M4 [Figure 3(a,d)] showed a smooth surface with no obviously pores, otherwise some pores existed in the surface of M2 and M3 [Figure 3(b,c)], whereas the pores in M2 seemed denser than M3. This result was in accordance with the packing density of M1, M3, and M4 shown in Table II that the samples with more pores have lower packing density. So, it could confirm that the pores were varied in the polymeric network of samples with the adding of different types of surfactant. As reported in the literature,²¹ pores in the surface could improve the contact area between polymeric network and external solution, and endow the samples with additional space to hold more water, which can facilitate the water absorption and swelling rate of PAA-Na resin.

From comparing Figure 3(e) with Figure 3(b), it shows much more pores as a result of adding the foam stabilizer TEA, which could increase the stability of foams so that to prolong the

existing time of bubbles, thus they could be wrapped in the polymeric network during the process of polymerization. Therefore, such a superior synergistic effect TEA with SBDS provides the resins lowest packing density according to the most pores, which contributes to the water absorption and the swelling rate of the SARs that have confirmed in the next description of “The influence of the packing density on the water absorption” and “The influence of the packing density on the swelling rate.”

The Influence of the Packing Density on the Water Absorption

Figure 4 shows the water absorption of M1, M2, M3, M4, and M5, it indicates that the packing density has a great influence on the water absorption of SARs. The water absorption order was: M2 > M3 > M1 > M4, which is indicated that lower packing density has higher water absorption. When adding different types of surfactant, the packing density is changed. Anionic or nonionic surfactant (M2 or M3) has decreased the packing density; however, cationic surfactant (M4) has a deterioration effect on it which has increased the packing density. This might be explained by the following reasons: (1) the surfactant can form a large amount of bubbles under stirring with eggbeater to introduce porous microstructure into the polymeric network in aqueous environment. The porosity reduces the packing density

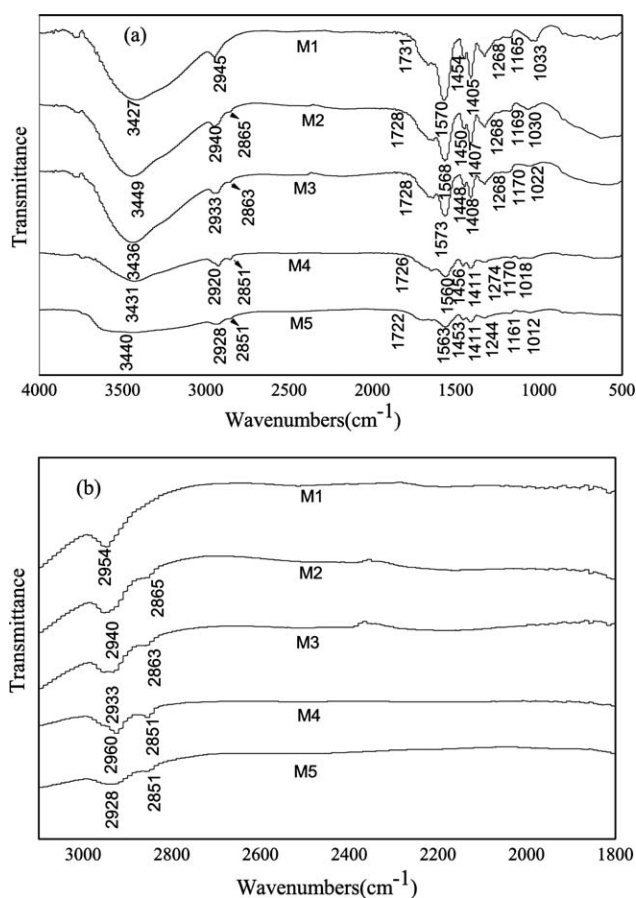


Figure 2. (a) FTIR spectra 4000 cm^{-1} to 500 cm^{-1} of washed M1, M2, M3, M4, and M5 and (b) the enlarged of FTIR spectra 3100 cm^{-1} to 1800 cm^{-1} of washed M1, M2, M3, M4, and M5.

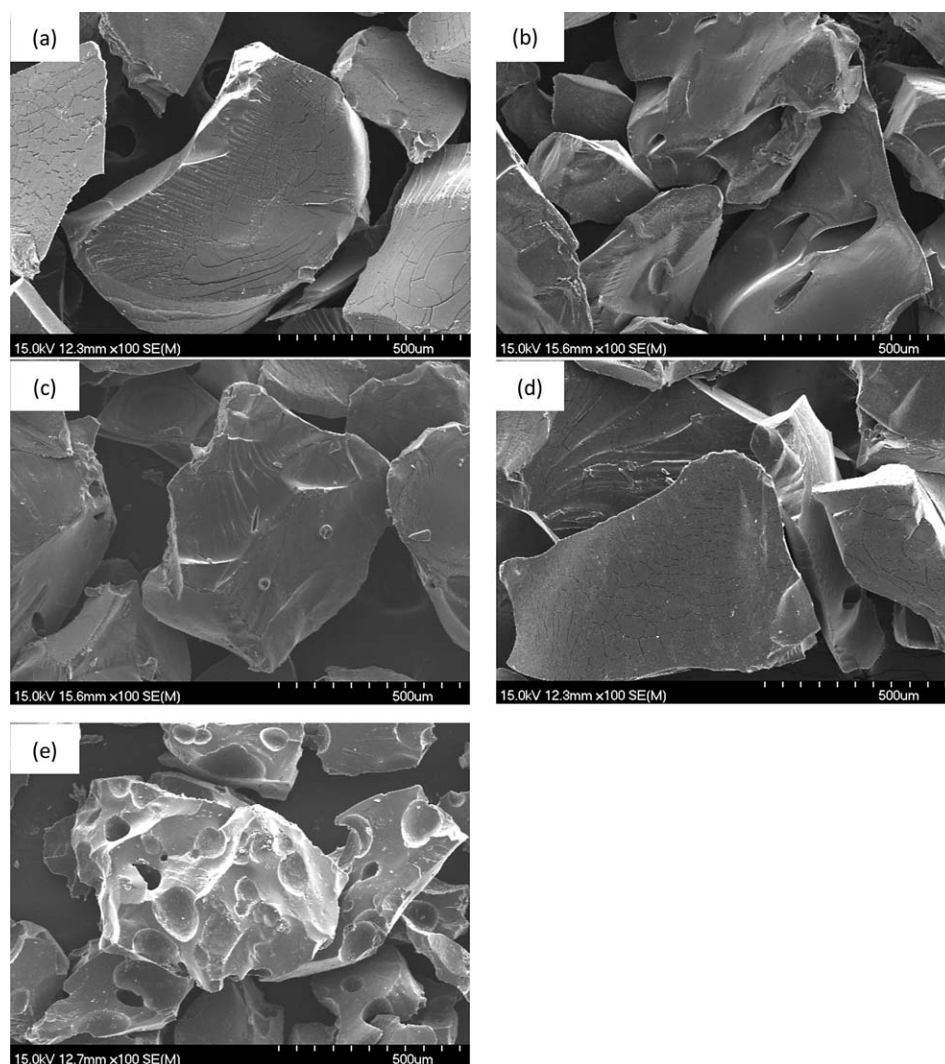


Figure 3. SEM images of PAA-Na resins (a) M1, (b) M2, (c) M3, (d) M4, and (e) M5.

(Table II) and plays multiple roles in enhancing the water absorption¹⁷ and the responsive rate of SARs; (2) the hydrophobic alkyl parts of surfactant could reduce the hydrogen-bonding interaction of polymeric chains, and also expand the network pore size. Accordingly, more water would be absorbed into the polymeric network.¹⁸ However, the water absorption with the addition of cationic surfactant CTAB (M4) was lower than non-surfactant sample (M1). This is may be due to the electrostatic attraction between the $-N^+(CH_3)_3$ ionized from CTAB with the $-COO^-$ of the reaction system during the polymerization process, which induced a light physical crosslinking in the hydrogel network,¹⁹ whereas pores in the surface disappeared and this was confirmed by the SEM images [Figure 3(d)] and the packing density was increased. While the electrostatic repulsion of the $-O-SO_3^-$ of SDBS molecules with the polyanionic chains in the crosslinking procedure is more inclined to the synergistic improvement of the porosity of the network, it decreases the packing density and increases the water absorption. Therefore, the water absorption of anionic SDBS-added was higher than that of nonionic OP-10-added and cationic CTAB-added samples.

Figure 4 shows that the water absorption of M5 is higher than M2. The stability of bubbles is dependent on the properties of foam film which is shown in Figure 1, such as the viscosity, strength, and so on. When adding the foam stabilizer TEA, it can form hydrogen bonds with the O atoms of SDBS to enhance the viscosity and strength of foam film. So adding TEA can substantially improve the foam stability, and high foam stability can prevent bubbles from destroying and more pores can be formed in the polymeric network. It results in slowing the rate of liquid loss through the foam film and reducing gas permeability. So the foam lifelong can be prolonged and the foam

Table II. The Packing Density of M1, M2, M3, M4, and M5

SARs	M1	M2	M3	M4	M5
m_2	3.70	3.51	3.59	3.82	3.40
ρ (g/mL)	0.84	0.79	0.81	0.87	0.76

Note: The known weight and volume container was 0.51 g and 3.8 mL, respectively.

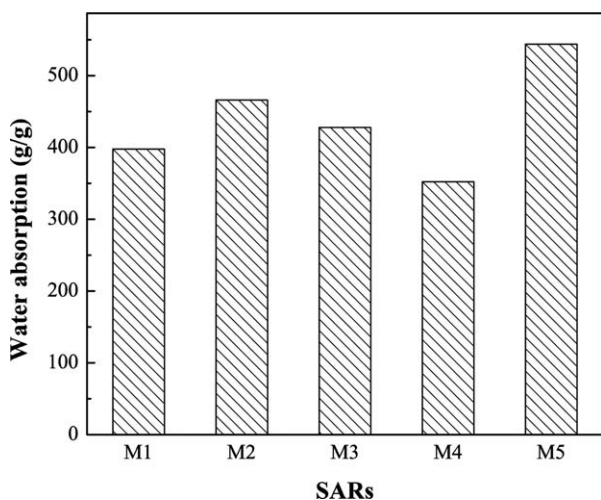


Figure 4. The water absorption of M1, M2, M3, M4, and M5.

stability is improved. Thus, the packing density is lower and the water absorption is higher of TEA with SDBS-added than that of only SDBS-added samples, as shown in Table II and Figure 4.

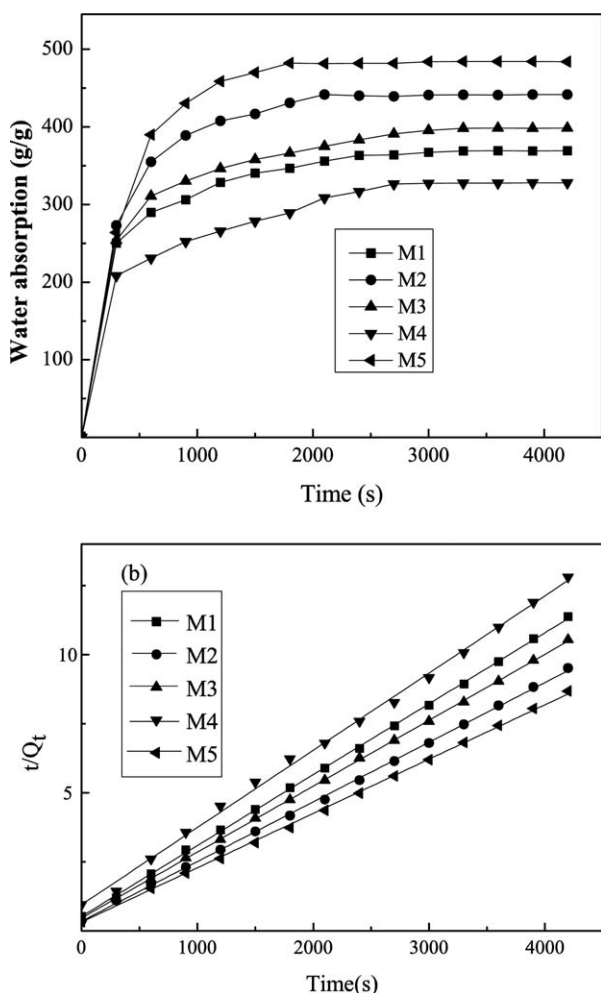


Figure 5. (a) The swelling kinetic curves and (b) t/Q_t versus t graphs of M1, M2, M3, M4, and M5.

Table III. Swelling Kinetic Parameters of M1, M2, M3, M4, and M5

SARs	Q_{eq} (g/g)	Q_{∞} (g/g)	k_{is} (g/g/s)
M1	369	389	1.91
M2	442	463	2.85
M3	398	418	2.15
M4	328	358	1.05
M5	484	508	3.12

The Influence of the Packing Density on the Swelling Rate

Besides the water absorbency of SARs, the swelling rate is also playing a key role in various application fields, such as biomedical, environmental, and pharmaceutical areas. The swelling rate of SARs is dependent on composition of polymers, the packing density and the external condition, and the influence of the packing density which depends on different types of surfactant. The system of foam stabilizer with surfactant on swelling rate is investigated in this section (Figure 5). Initially, the swelling rate increases and then begins to level off after 800 s until the equilibrium swelling is achieved. The effect of the packing density of the samples on the swelling kinetic behaviors analyzed by a Schott's pseudo second-order swelling kinetics model²⁰ (3):

$$\frac{t}{Q_t} = \frac{1}{k_{is}} + \frac{1}{Q_{\infty}} t \quad (3)$$

where Q_t is the water absorption at time t , Q_{∞} is the theoretical equilibrium water absorption, and k_{is} is the initial swelling rate constant. Graphs of t/Q_t versus t give straight lines with relative good liner correlation coefficient, indicating that the swelling rate of samples obeys the Schott's theoretical model. The swelling parameters such as k_{is} and Q_{∞} can be calculated by the intercept and slope of lines and are presented in Table III.

Figure 5 shows the swelling behavior of M1, M2, M3, M4, and M5 samples. Comparing with M1, M2, M3, and M4, we can see that the swelling rate of the resins in distilled water is varied with altering the packing density of the resins. The packing density is changed with the addition of surfactants. The addition of proper amount of SDBS and OP-10 gives rise to the initial absorption rate through the generation of porous microstructure in the three-dimensional polymeric network. However, in the case of cationic surfactant CTAB, the electrostatic attractive forces between the carboxylate ions ($-\text{COO}^-$) of anionic polymer chains and ammonium ions ($-\text{N}^+(\text{CH}_3)_3$) of CTAB molecules result in almost no pores on the surface of M4 [as shown in Figure 3(d)] and slight physical crosslinking in the polymeric network, which reduce the free space network, increase the packing density, and slow the diffusion of water molecules into the samples.

The comparison between M2 and M5 in Figure 5 shows that adding foam stabilizer could significantly improve the foam stability, make the foam surface denser, increase the surface elasticity, and decrease the volume of single bubble which became more uniform and small, so that the foams were difficult to break. Therefore, as depicted above, M5 had more foams formed in the polymeric network, more pores on the surface [as shown in Figure 3(f)] which leads to lower packing density

(Table II). Moreover, lower packing density facilitates the water molecules to enter the polymeric network more easily and contributes to enlarge surface area to speed up the diffusion rate of water molecules and improve the swelling rate of the samples.

CONCLUSIONS

The superabsorbent PAA-Na resins was prepared by a free radical solution polymerization reaction, using a self-assembled micelle of surfactant as a blowing agent to achieve a porous microstructure for decreasing the packing density. Furthermore, the water absorption and swelling rate is enhanced. In the case of fiercely stirring by eggbeater, the action of the surfactant formed a large number of bubbles, and then the bubbles were enshrouded in the polymeric network of the resins during the process of polymerization reaction, so a porous superabsorbent PAA-Na resin was prepared. The experimental results proved that using the anionic and nonionic surfactants could reduce the packing density, and then improve both the water absorption and swelling rate, because they could form effective pores to increase the surface area and change the way of resins absorbing water, which is from diffusion into combined effect of diffusion and capillary. Among these types of surfactant, the anionic surfactant has the largest influence on the porous microstructure, which is attributed to the electrostatic repulsion existing between in the anionic surfactant molecules and carboxylate ions of polyanionic chains that could effectively expand the polymeric network size. While the cationic surfactant has negative effect on porous microstructure due to the electrostatic attraction between the surfactant and polymer chains, so that it has highest packing density and worst water absorbing capacity. Furthermore, the foam stabilizer TEA with the surfactant SDBS could form viscoelasticity foam film to prevent the formed bubbles to disappear, and prolong the lifetime of foams that is because TEA can form hydrogen bonds with the O atoms of SDBS, which could produce more pores in the polymeric network than only surfactants were used. Hence, adding foam stabilizer with surfactant could dramatically decrease the packing density and increase the water absorbency. Therefore, we used the special synergistic effect of the system of surfactant and foam stabilizer, and it has dramatically influence on reducing the packing density, improving the water absorption, and swelling rate of superabsorbent PAA-Na resins.

ACKNOWLEDGMENTS

This work was financially supported by Major Science and Technology Project of Zhejiang Province (No. 2011C01004), Zhejiang

Provincial Natural Science Foundation of China (Grant No. LY14E030003, LY14E030004).

REFERENCES

1. Zohuriaan-Mehr, M. J.; Kabiri, K. *Iran. Polym. J.* **2008**, *17*, 451.
2. Omidian, H.; Rocca, J. G.; Park, K. *J. Controlled Release* **2005**, *102*, 3.
3. Zhang, B. N.; Cui, Y. D.; Yin, G. Q.; Li, X. M.; Liao, L. W.; Cai, X. B. *Polym. Compos.* **2011**, *32*, 683.
4. Wang, W. B.; Wang, A. Q. *Carbohydr. Polym.* **2010**, *82*, 83.
5. Seetapan, N.; Srisithipantakul, N.; Kiathamjornwong, S. *Polym. Eng. Sci.* **2011**, *51*, 764.
6. Chen, J.; Park, H.; Park, K. *J. Biomed. Mater. Res.* **1999**, *44*, 53.
7. Gotoh, T.; Nakatani, Y.; Sakohara, S. *J. Appl. Polym. Sci.* **1998**, *69*, 895.
8. Kato, N.; Sakai, Y.; Shibata, S. *Macromolecules* **2003**, *36*, 961.
9. Wu, F.; Liu, C. S.; O'Neill, B.; Wei, J.; Ngothai, Y. *Appl. Surf. Sci.* **2012**, *258*, 7589.
10. Varaprasad, K.; Ravindra, S.; Reddy, N. N.; Vimala, K.; Raju, K. M. *J. Appl. Polym. Sci.* **2010**, *116*, 3593.
11. Regismond, S. T. A.; Gracie, K. D.; Winnik, F. M.; Goddard, E. D. *Langmuir* **1997**, *13*, 5558.
12. Antonietti, M.; Caruso, R. A.; Goltner, C. G.; Weissenberger, M. C. *Macromolecules* **1999**, *32*, 1383.
13. Von Klitzing, R. *Adv. Colloid Interface Sci.* **2005**, *114*, 253.
14. Taylor, D. J. F.; Thomas, R. K.; Penfold, J. *Adv. Colloid Interface Sci.* **2007**, *132*, 69.
15. Rao, A.; Kim, J. D.; Thomas, R. R. *Langmuir* **2005**, *21*, 617.
16. Li, W.; Wang, J. L.; Zou, L. H.; Zhu, S. Q. *Eur. Polym. J.* **2008**, *44*, 3688.
17. Chen, J.; Park, K. *Carbohydr. Polym.* **2000**, *41*, 259.
18. Zhang, J. P.; Chen, H.; Li, P.; Wang, A. Q. *Macromol. Mater. Eng.* **2006**, *291*, 1529.
19. Nystrom, B.; Roots, J.; Carlsson, A.; Lindman, B. *Polymer* **1992**, *33*, 2875.
20. Schott, H. *J. Macromol. Sci. Phys.* **1992**, *31*, 1.
21. Hu, X. Y.; Li, Y.; He, X. J.; Li, C. X.; Li, Z. Q.; Cao, X. L.; Xin, X.; Somasundaran, P. *J. Phys. Chem. B* **2012**, *116*, 160.